Studies of Pure- and Aerated-Liquid Jets Using the X-Ray Phase Contrast Imaging

K.-C. Lin*
Taitech, Inc.
Beavercreek, Ohio 45430

Campbell Carter
Air Force Research Laboratory, Propulsion Directorate
Wright-Patterson AFB, Ohio 45433

Kamel Fezzaa, Zunping Liu, Jin Wang
Argonne National Laboratory

Abstract

The structures of pure- and aerated-liquid jets injected into a quiescent environment were investigated, using the phase contrast imaging technique combined with an x-ray light source. The experiment was carried out at the 32-ID Beamline at the Argonne National Laboratory. Water and nitrogen were used as the injectant and aerating gas, respectively. Two aerated-liquid injectors with orifice diameters of 0.5 and 1.0 mm were utilized for liquid injection. Pure-liquid jets were generated by turning off the aerating gas supply. It was found that the x-ray phase contrast imaging provides the unique capability of depicting line-of-sight interfacial features on the entire periphery of the liquid column, ligament, and droplet. Highly convoluted wrinkle structures on the column surface of a turbulent pure-liquid jet were observed. The length scale of the wrinkle structures decreases as the liquid flow rate, liquid Reynolds number or liquid Weber number increases. The near-field structures of aerated-liquid jets, which are optically dense, can be clearly depicted by using the present diagnostic technique. With a modest level of liquid aeration, the liquid column can be dispersed into fine droplets and ligaments inside the injector. The entrained gas inside the droplets and ligaments of aerated-liquid jets expands into bubbles, which can be clearly observed in the x-ray images. The entrained gas eventually bursts to generate fine droplets at downstream locations. Increase in aeration level enhances liquid atomization.

Introduction

Liquid jets atomized in a high-speed air crossflow environment play an important role in establishing stable and efficient combustion within the extremely limited distance and time scale inside the combustor of a liquid-fueled air-breathing propulsion system. In order to produce deeper fuel penetration into the air stream for broader fuel spreading, and to generate smaller droplets in the liquid spray for faster evaporation, a superior liquid injection scheme must be sought. Among the possible candidates, aerated-liquid (or effervescent, or barbotage) jets have been explored extensively. Its favorable characteristics for high-speed air-breathing propulsion application, including deep penetration, a large fuel plume, small droplet size, and high droplet number density, have been illustrated [1,2]. The utilization of aerated-liquid jets has also led to successful combustion in a liquid-fueled high-speed air-breathing combustor [3].

While the general features of the aerated-liquid jets are very promising, detailed near-field spray structures, such as the liquid disintegration process and the distributions of droplet properties and liquid volume flux within the jets, cannot be easily obtained, due to instrumentation difficulties. The relatively dense spray structure, along with high gas and droplet velocities, make conventional diagnostics, such as shadowgraph imaging and phase Doppler particle analyzer (PDPA), either inapplicable or unreliable. The holographic technique has been successfully utilized to measure droplet size and velocity in the vicinity of the near-field jet [4]. This technique, however, has not been applied to the exploration of the interior structures of near-field aerated-liquid jets. Figure 1 illustrates the appearance of pure- and aerated-liquid jets injected into a subsonic crossflow. The extremely dense structure of the aerated-liquid jets in the directly-illuminated photo pictures in Figure 1 highlights the difficulties in exploring the near-field structures, which dictate the subsequent spray structures and droplet properties. Advanced diagnostic tech-

*Corresponding author, Kuo-Cheng.Lin@wpafb.af.mil

niques are, therefore, needed, in order to further advance the understanding of the aerated-liquid jets. The candidate diagnostic technique should create a relatively small light scattering pattern for a dense spray in order to "see through" the dense structures. The x-ray facility at the Argonne National Laboratory provides the ideal light source and was, therefore, utilized for the present study [5,6].

The objective of this study is to experimentally investigate the near-field structures of pure- and aerated-liquid jets injected into a quiescent environment, using the phase contrast imaging technique combined with the x-ray light source at the Argonne National Laboratory. Unique surface structures of the pure-liquid jets and the effects of liquid aeration on liquid atomization will be qualitatively discussed.

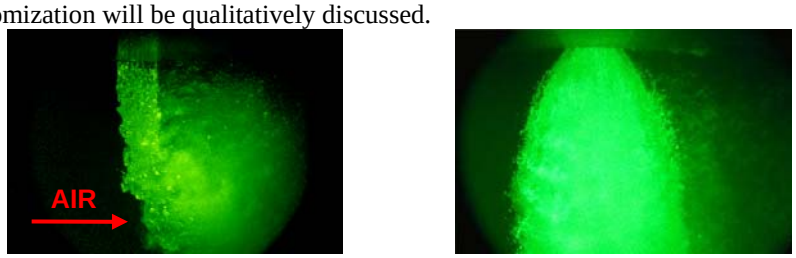

(a) GLR=0% (b) GLR=8.0%

Figure 1. Photographs of near-field structures of water jets injected from the top of the image into a subsonic environment at various aeration levels: (a) Pure-liquid jet, (b) Aerated-liquid jet. M_∞=0.3, d=1.0 mm, q_0=10.4. The jets were illuminated with a 7-ns pulse laser beam from an Nd-YAG laser.

Experimental Methods

The experiment was conducted at the XOR 32-ID beamline of the Advanced Photon Source (APS) at the Argonne National Laboratory. The undulator source provides the high x-ray brilliance necessary for the white-beam ultra-fast imaging technique. With the undulator gap set to 31 mm, most of the intensity was located within the first harmonic at 13.3 keV, with a peak irradiance of 10^{14} ph/s/mm^2/0.1%bw and a natural 5 bandwidth of 0.3 keV at FWHM. For imaging of the liquid jet, the higher order harmonic was used and the lower energy was filtered with a 10 mm thick silicon slab. A fast scintillator crystal (LYSO:Ce, with a 40 ns decay time) converted the transmitted x-rays into visible light (434 nm). The images were captured with a fast CCD camera (Sensicam HS-SVGA, 1024×1280 pixels, from Cooke Corp.) coupled to the scintillator via a microscope objective (5x, NA = 0.14) and a 45º mirror. The field of view of the imaging system (1.3 × 1.7 mm^2) matched the full usable x-ray beam size. The ultrafast imaging capability of the present setup provides an exposure time of 170 ps for each image. Originally, the structures of aerated-liquid jets both inside the injector and immediately after injection were to be probed by the x-ray. Attempts to image the structure of the two-phase mixture inside the injector, however, were unsuccessful. The instantaneous image of the fast-moving two-phase mixture inside the injector could not be captured in the 5-μs exposure time, which is required for a higher energy x-ray to penetrate the injector metal walls. Therefore, the present study focuses on the structures of liquid jets immediately downstream of the injector orifice.

Water and nitrogen were supplied into the aerated-liquid injector at desired flowrates to form a two-phase mixture prior to discharging into a quiescent environment. Two aerated-liquid injectors with discharge orifices of 0.5 and 1.0 mm were utilized for the present study. The aerated-liquid jet was vertically discharged into a collecting bucket with a small opening on the cap to prevent drifted droplets getting into the beam path. In addition, the distance between the nozzle exit and the bucket cap was kept at 10 mm, in order to avoid water splashing. Both the aerated-liquid injector and the collecting bucket were rigidly mounted on a traversing table, which provides desired movement normal to the x-ray beam.

Results and Discussion

Pure-Liquid Jets

Figure 2 shows the composite x-ray images of pure-liquid jets injected from a 1.0-mm aerated-liquid injector at various liquid flow rates. The images for each jet were not taken at the same time instance. The Reynolds number and Weber number range from 1.19×10^4 to 4.02×10^4 and from 2.1×10^3 to 23.8×10^3 for those four jets, respectively. The injected flows are all turbulent, since the Re number is greater than 4,000. Also, the emerging flows are fully-developed pipe flows. The physical dimension of the jet is 9.4 mm in the injection direction. These images show that the highly-convoluted surface structures along the periphery of the liquid jet can be clearly visualized by the line-of-sight x-ray. These surface features have never been seen before. The combination of the phase contrast imaging technique and the unique properties of the x-ray provides the capability to depict subtle variation in surface continuity over the entire periphery of the liquid jet.

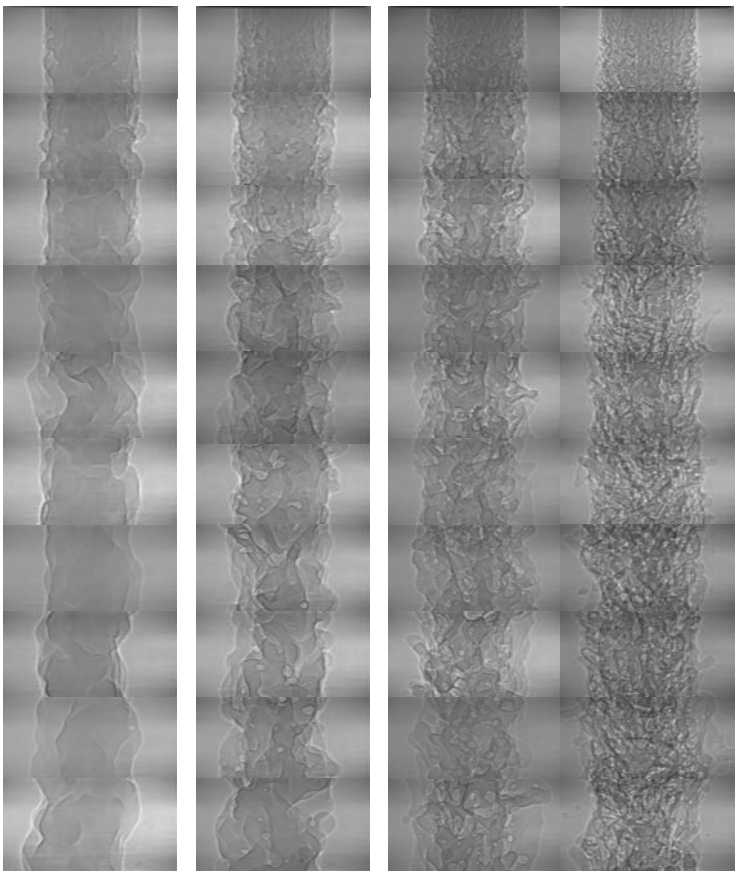

Figure 2. Composite x-ray images of pure-liquid jets injected into a quiescent environment at various liquid flow rates. d=1.0 mm. The physical dimension in the vertical direction is 9.4 mm. (a) Q_L=0.58 l/min (We=2.1×10^3, Re=1.19×10^4), (b) Q_L=1.03 l/min (We=6.6×10^3, Re=2.12×10^4), (c) Q_L=1.36 l/min (We=11.4×10^3, Re=2.80×10^4), (d) Q_L=1.95 l/min (We=23.8×10^3, Re=4.02×10^4).

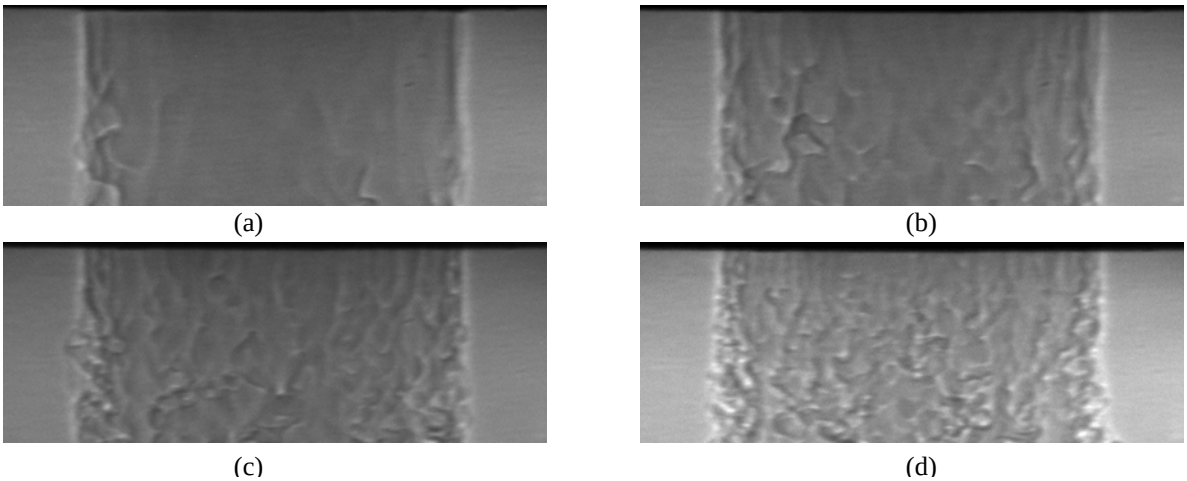

Figure 3. X-ray images of pure-liquid jets adjacent to the nozzle exit. d=1.0 mm. The physical dimension in the vertical direction is 0.5 mm. (a) Q_L=0.58 l/min (We=2.1×10^3, Re=1.19×10^4), (b) Q_L=1.03 l/min (We=6.6×10^3, Re=2.12×10^4), (c) Q_L=1.36 l/min (We=11.4×10^3, Re=2.80×10^{44}), (d) Q_L=1.95 l/min (We=23.8×10^3, Re=4.02×10^4).

Based on the appearances, the wrinkle structure is related to the combined effect of turbulence eddies within the liquid jet and the shear force interaction between the high-speed liquid and quiescent air. Please note that the x-ray

image is line of sight. The actual density of the wrinkle structure on the jet surface is one half of the density observed in Figure 2. If conventional shadowgraph images were used for the study, the wrinkle structures at the surfaces tangential to the parallel light would strongly resemble surface waves. According to the numerical study by Pai et al. [7], the length scale of the wrinkle structure is mainly a function of the jet We number. As the liquid flow rate or Weber number increases from Figure 2(a) to Figure 2(d), the observed length scale clearly decreases.

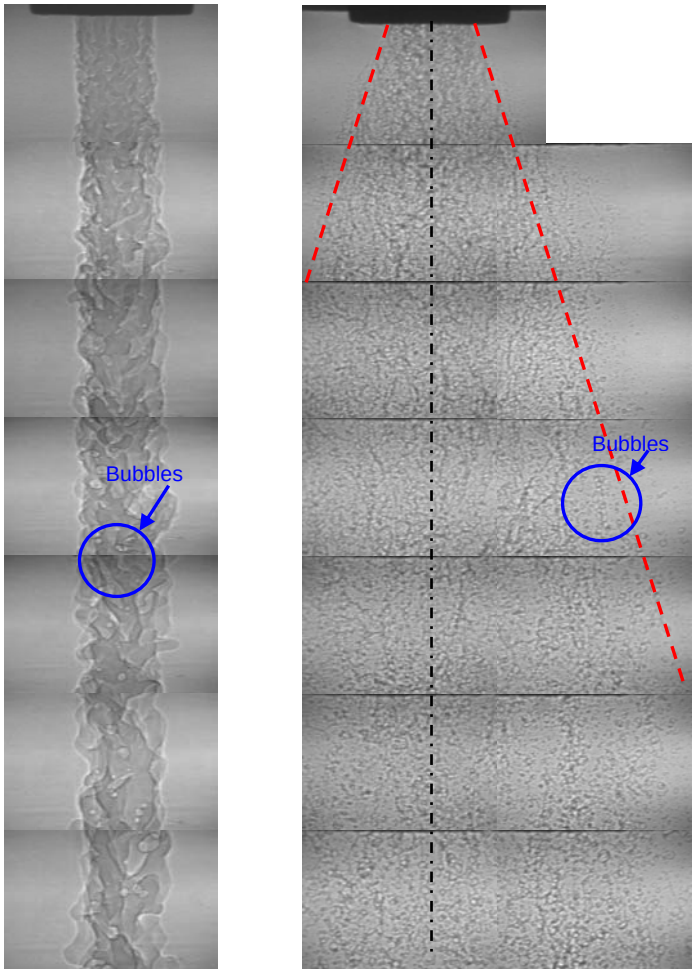

Figure 4. Composite x-ray images of pure- and aerated-liquid jets injected into a quiescent environment. d=0.5 mm, Q_L=0.53 l/min (Re=2.18×10^4). The physical dimension for the liquid jet in the vertical direction is 6.1 mm. (a) GLR=0 (b) GLR=1.41%.

Figure 2(a) also shows that the length scale of the wrinkle structure increases with streamwise distance, probably due to the dissipation of the small wrinkle structures, similar to the dissipation of small turbulence eddies, or due to the growth of surface waves induced by Kelvin-Helmholtz instability. The same phenomena can be observed for the jet in Figure 2(b). For the high Re (or We) jet in Figure 2(d), there are high-density small turbulence eddies on the jet surface. Some protruding ligaments and stripped drops can be seen along the jet edges. The high-density wrinkle structures do not dissipate within the probing area for this jet.

Figure 3 shows blown-up x-ray images for the four pure-liquid jets in Figure 2 within 0.5 mm from the nozzle exit. Careful examination of Figure 3 shows that there exist elongated surface structures adjacent to the nozzle exit. These structures are orientated with the jet injection direction. Both length and width of the elongated structure decrease as the jet Re (or We) number increases. These elongated structures transform into small three-dimensional wrinkle structures, which gradually grow into the bigger structures at downstream locations. Based on the study by Ganapathisubramani et al. [8], the elongated structures come from the velocity gradients inside the injector wall boundary layer. Elongated regions of uniform momentum with a length greater than 8 times the boundary layer

thickness were recently observed inside a supersonic turbulent boundary layer over a flat plate [8]. The orientation of these elongated structures is also aligned with the freestream flow.

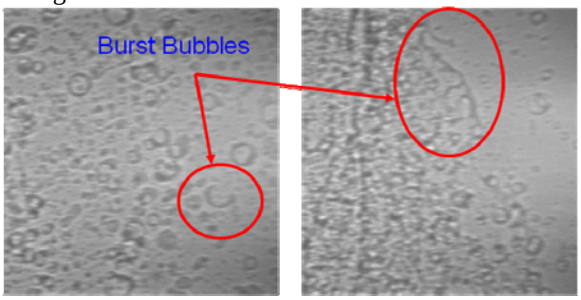

Figure 5. X-ray images of aerated-liquid jets to illustrate bubble burst.

Aerated-Liquid Jets

The effect of liquid aeration on the destruction of the liquid column can be easily seen by comparing the pure- and aerated-liquid jets in Figure 4, where the liquid is water and the aerating gas is nitrogen. The same liquid flow rate was injected from a 0.5-mm injector. In the pure-liquid jet in Figure 4(a) the liquid column is still intact within the field of view. The general features of the pure-liquid jet are similar to those observed in Figure 2. Please note that gas bubbles, which may come from the residue gas inside the aerating gas chamber, are embedded inside the liquid column and can be clearly seen in the x-ray images. Once again, the combination of the phase contrast imaging technique and the x-ray provides the capability to depict the interface of the gas bubble inside the liquid column. The gas bubble grows in size as it moves downstream and experiences pressure relaxation.

In the aerated-liquid jet in Figure 4(b), which has a gas-to-liquid mass ratio (GLR) of 1.41%, the injected jet is already disintegrated into small droplets and fine ligaments immediately after injection. No intact liquid core can be observed at this aeration level. The advantage of liquid aeration in enhancing the liquid atomization processes is quite obvious. The two-phase mixture generated from the internal mixing of water and nitrogen is nearly a homogeneous mixture. With a slightly higher injection pressure, the injected two-phase mixture exhibits a larger spreading angle. The advantage of using the x-ray technique can also be seen between Figure 1(b) and Figure 4(b). In the image in Figure 4(b) the small droplets and fine ligaments are discernible. The droplets and ligaments are, however, highly clustered at the central region of the jet close to the jet exit, due to the high number density at this axial location and the line-of-sight nature of the x-ray image.

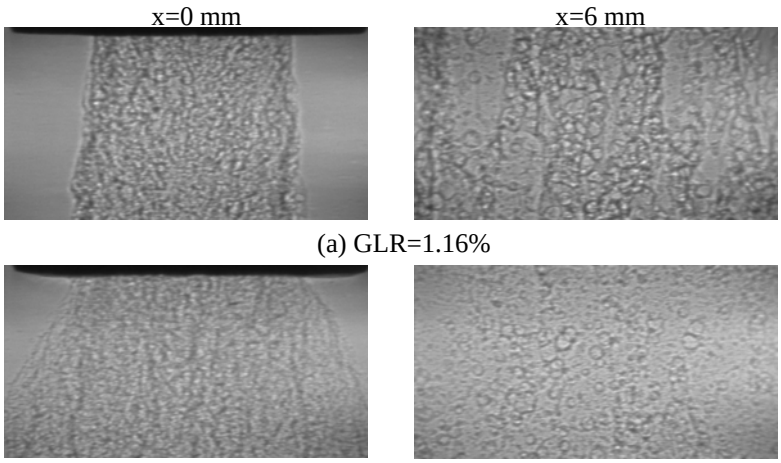

(a) GLR=1.16%

(b) GLR=4.13%

Figure 6. X-ray images of an aerated-liquid jet injected into a quiescent environment at two downstream locations. d=1.0 mm, Q_L=0.64 l/min. (a) GLR=1.16%, (b) GLR=4.13%

With the present diagnostic technique, tiny bubbles are observed embedded inside some droplets and ligaments at downstream locations in the aerated-liquid jet. Apparently, some aerating gas gets entrained into the liquid during the mixing process inside the aerated-liquid injector and expands into bubbles as the entrained gas experiences pressure relaxation at the downstream locations. That is also the reason why some bigger droplets, which actually have

hollow structures, can be observed at the downstream locations. Eventually, these gas bubbles burst to generate fine droplets at further downstream locations, as illustrated in Figure 5.

Figure 6 illustrate the effects of liquid aeration on atomization processes. The liquid flow rate was kept the same in both injection conditions. For the GLR=1.16% jet, the x-ray image shows that streams of gas bubbles are mainly entrained inside the ligaments. Please note the existence of smaller droplets surrounding the bubble-embedded ligaments at x=6 mm locations for both jets. These droplets contain no entrained gas and may potentially collide with the expanded ligaments. With a higher injection pressure, the case with GLR=4.13% exhibits a wider jet expansion at nozzle exit. With an improved liquid dispersion for the GLR=4.13% jet, there are more fine droplets and fewer bubble-embedded ligaments within the field of view at the x=6 mm location. The degree of liquid dispersion appears to increase with liquid aeration.

Conclusions

The structures of pure- and aerated-liquid jets injected into a quiescent environment were explored, using the phase contrast imaging technique combined with the x-ray light source. Never-before-seen features on the liquid column surface of the pure-liquid jets were observed and qualitatively described. In addition, near-field structures of the aerated-liquid jets and the advantages of liquid aeration were discussed. The x-ray phase contrast imaging provides the unique capability of depicting interfacial features on the entire periphery of the liquid column, ligament, and droplets. With the present diagnostic technique, highly-convoluted wrinkle structures on the column surface of a turbulent liquid jet were observed. The length scale of the wrinkle structures decreases as the liquid flow rate or liquid Weber number increases. The near-field structures of aerated-liquid jets, which are optically dense, can be clearly depicted by the present diagnostic technique. With a modest level of liquid aeration, the liquid column can be dispersed into fine droplets and ligaments, which can contain entrained gas. The entrained gas inside the droplets and ligaments of aerated-liquid jets expands into bubbles and eventually bursts to generate fine droplets as the gas bubbles experience pressure relaxation at downstream locations. Increase in aeration level enhances liquid atomization.

Nomenclature

d	= injector orifice diameter
GLR	= aerating gas-to-liquid mass ratio
M_∞	= freestream Mach number
Q_L	= liquid volumetric flow rate
q_0	= jet-to-air momentum flux ratio at GLR=0
Re	= Reynolds number
We	=. Weber number
x	= axial position downstream of the injector exit centerline

Acknowledgements

Financial support from AFRL/Propulsion Directorate and facility support from Advance Photon Source at the Argonne National Laboratory are acknowledged.

References

1. Lin, K.-C., Kennedy, P. J., and Jackson, T. A., “Spray Structures of Aerated-Liquid Jets in Subsonic Crossflows,” AIAA Paper 2001-0330, 2001.
2. Lin, K.-C., Kennedy, P. J., and Jackson, T. A., “Structures of Aerated Liquid Jets in High Speed Crossflows,” AIAA Paper 2002-3178, 2002.
3. Mathur, T., Lin, K.-C., Kennedy, P., Gruber, M., Donbar, J., Jackson, T., and Billig, F., “Liquid JP-7 Combustion in a Scramjet Combustor,” AIAA Paper 2000-3581, July, 2000.
4. Sallam, K. A., Aalburg, C., Faeth, G. M., Lin, K.-C., Carter, C. D., and Jackson, T. A., “Primary Breakup of Round Aerated-Liquid Jets in Supersonic Crossflows,” *Atomization and Sprays*, Vol. 16, No. 6, 2006, pp. 657–672.
5. Wang, Y., Liu, X., Im, K.-S., Lee, W.-K., Wang, J., Fezzaa, K., Hung, David, and Winkelman, J., “Ultrafast X-Ray Study of Dense Liquid Jet Flow Dynamics Using Structure Tracking Velocimetry,” *Nature Physics* (accepted).
6. Qun, S., Lee, W-K., Fezzaa, K., Chu, Y. S., De Carlo, F., Jemian, P., Ilavsky, J., Erdman, M., and Long, G., “Dedicated Full-Field X-Ray Imaging Beamline at Advanced Photon Source,” *NIM A* 582 (1), 77-79 (2007).
7. Pai, M., Pitsch, H., and Desjardins, O., “Detailed Numerical Simulations of Promary Atomization of Liquid Jets in Crossflow,” AIAA Paper 2009-0373, January, 2009.
8. Ganapathisubramani, B., Clemens, N. T., and Dolling, D. S., “Large Scale Motion in a Supersonic Turbulent Boundary Layer,” *J. Fluid Mech.*, Vol. 556, 2006, pp. 271-282.